Thin Solid Films 518 (2010) 5173–5176

Contents lists available at ScienceDirect

Thin Solid Films

journal homepage: www.elsevier.com/locate/tsf

Epitaxial EuO thin films by pulsed laser deposition monitored by *in situ* x-ray photoelectron spectroscopy

J.N. Beukers *, J.E. Kleibeuker, G. Koster, D.H.A. Blank, G. Rijnders, H. Hilgenkamp, A. Brinkman

Faculty of Science and Technology and MESA+ Institute for Nanotechnology, University of Twente, 7500 AE Enschede, The Netherlands

ARTICLE INFO

Article history:
Received 23 December 2009
Received in revised form 22 April 2010
Accepted 27 April 2010
Available online 10 May 2010

Keywords:
EuO
Ferromagnetic insulators
Pulsed laser deposition
X-ray photoelectron spectroscopy

ABSTRACT

We have grown EuO thin films on silicon [001] and yttrium aluminate [110] from a europium metal target using pulsed laser deposition. *In situ* x-ray photoelectron spectroscopy has been used to determine the parameter window for stoichiometric EuO deposition. EuO is observed to grow in the relatively high pressure regime of 10^{-6}–10^{-5} mbar, due to the large Eu flux during ablation. EuO is proven to grow epitaxially on yttrium aluminate [110]. Magnetization measurements confirm the stoichiometry of the film.

1. Introduction

EuO is a promising material in the fields of solid state quantum information processing and spintronics. EuO is a ferromagnetic semiconductor with a Curie temperature (T_C) of 70 K and a bandgap of 1.12 eV. A great challenge in spintronics is to realize fully spin polarized current injection into metallic or semiconducting electrodes. A possible realization is by injection through spin selective tunnel barriers such as dilute magnetic semiconductors [1] and semiconductors which exhibit inherent magnetic ordering, such as the europium chalcogens [2,3] and specifically EuO [4,5]. The spin-selectivity of EuO barriers arises from the Zeeman splitting of the conduction band [6,7], providing a different barrier height for each spin population. Additionally, this principle can be applied to spin measurement devices [8].

When electron doped, either by creating oxygen vacancies or by replacing some of the Eu^{2+} ions by trivalent rare earth elements, the conductivity of EuO can be tuned over many orders of magnitude, while preserving its large degree of spin-polarization [9,10]. Although the magnetoresistance is not as large as the collosal magnetoresistance in the manganites [11,12], exceptionally large magnetoresistance was observed near the metal-to-insulator transition in doped EuO [7].

Over the last decade, EuO thin film growth techniques have been developed on the basis of molecular beam epitaxy (MBE) [4–6,9,10,13–15]. Possible substrate materials include Si [9,10], yttrium aluminate ($YAlO_3$) and GaN [9]. At low deposition temperatures, the stoichiometry of the $EuO_{1\pm\delta}$ during MBE growth needs to be tuned by a careful matching of the europium and oxygen fluxes. A too high oxygen pressure will result in the incorporation of the more stable oxides Eu_3O_4 and Eu_2O_3 in the film, while too low oxygen reactivity gives rise to oxygen vacancies in the film that effectively dope charge carriers into EuO. At elevated deposition temperatures an alternative absorption controlled growth regime is accessible because of the re-evaporation of surplus Eu at the surface [15]. With a Eu flux that is typical for MBE [4,6,9,15–17] (about 10^{13}–10^{14} atoms/cm^2 s) the stability window is reported to be in the oxygen partial pressure range of 10^{-8} mbar [15].

In this article, we present the realization of epitaxial EuO thin films by PLD on $YAlO_3$ [110] and stoichiometric, poly-crystalline films on Si [001]. Correct stoichiometry is demonstrated by x-ray photoelectron spectroscopy and magnetization measurements.

With pulsed laser deposition (PLD), nanosecond pulses locally heat the target surface, causing ablation of target material in the order of 10^{16} atoms per pulse in the case of an europium metal target. PLD is a potentially interesting EuO deposition technique since the time averaged flux is up to 2 orders of magnitude larger than in the case of MBE and can be increased by increasing the ablation frequency. This implies that the window for stoichiometric EuO deposition shifts toward higher oxygen pressures, as indicated in Fig. 1, enabling the use of more accessible high vacuum (HV) systems instead of ultra-high vacuum (UHV) deposition chambers. Moreover, the europium flux can be altered easily with PLD by adjusting the deposition frequency. Furthermore, PLD is a versatile and widely used deposition technique, which allows, for example, for an easy integration with the deposition of other complex oxide materials. An example of such an experiment is $LaAlO_3$ on EuO.

---

* Corresponding author.
E-mail address: j.n.beukers@tnw.utwente.nl (J.N. Beukers).

0040-6090/$ – see front matter © 2010 Elsevier B.V. All rights reserved.
doi:10.1016/j.tsf.2010.04.071

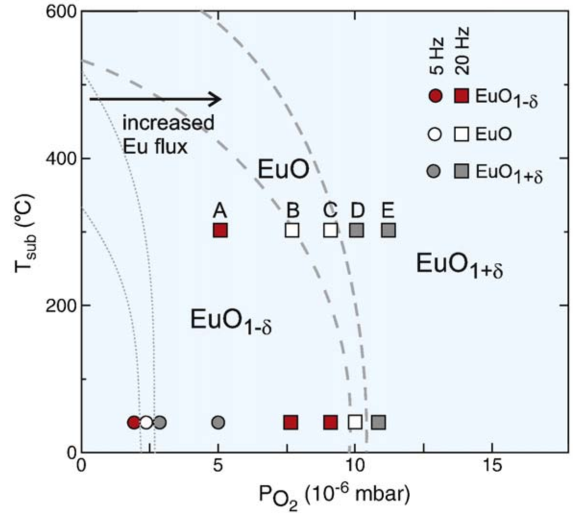

Fig. 1. Schematic representation of the phase diagram of $EuO_{1\pm\delta}$ deposited by PLD. The stability window, in which EuO forms, shifts as function of ablation frequency. The data points correspond to ablation frequencies of 5 and 20 Hz. The squares marked A to E correspond to the XPS spectra of Fig. 2. The shape of the stability window, depicted with the dashed and dotted lines, can roughly be constructed from MBE deposition conditions [4,6,9,15].

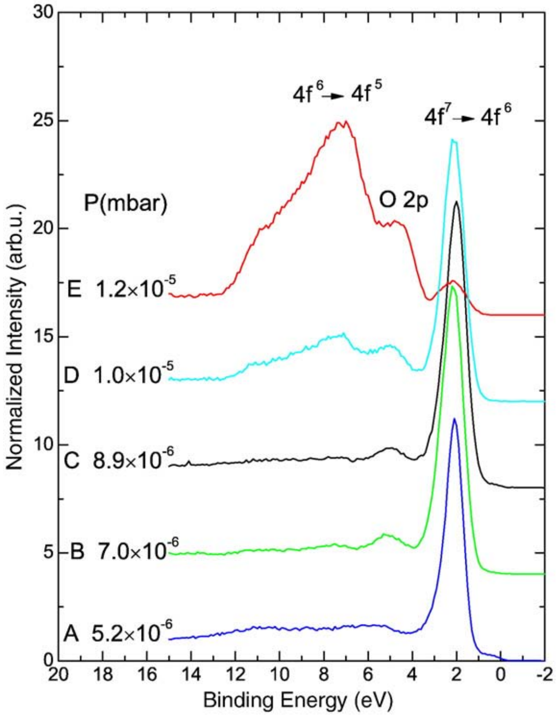

Fig. 2. *In situ* XPS valence band spectra ($h\nu = 1485$ eV) of a Eu film (A) and 4 different $EuO_{1\pm\delta}$ thin films (B, C, D and E) deposited on Si. Film A is deposited at 300 °C in 5.2×10^{-6} mbar of oxygen with an ablation frequency of 20 Hz. Films B to E are deposited under the same conditions in increasing oxygen partial pressures up to 1.2×10^{-5} mbar.

Polar reconstruction at this interface is expected to give a spin polarized two dimensional electron gas [18].

2. *In situ* x-ray photoelectron spectroscopy on EuO thin films

In order to determine the position of the stoichiometric EuO stability window during PLD, initial experiments were carried out in an UHV PLD chamber with a base pressure below 10^{-8} mbar, equipped with *in situ* x-ray and ultraviolet photo emission spectroscopy (XPS, UPS) tools. The XPS measurements were done using a monochromated Al source. XPS is a powerful tool for determining the stoichiometry in EuO since oxygen deficient films give a detectable Fermi edge in the valence band spectrum and oxygen rich films give a detectable Eu^{3+} contribution to the spectrum.

Si [001] substrates were pre-treated with 1% HF in water to remove the native oxide layer. The substrate temperature is varied between room temperature (RT) and 300 °C. In these experiments europium is ablated from a europium metal target using a KrF ($\lambda = 248$ nm) laser. The applied fluence is 2 J cm^{-2} and the deposition frequency is varied between 5 and 20 Hz.

Europium is ablated in an oxygen partial pressure ranging between 1×10^{-7} and 1.2×10^{-5} mbar, measured with an ion gauge. The pressure is controlled by a needle valve. In order to construct a phase diagram, depositions at an ablation frequency of 5 and 20 Hz were done. Fig. 1 shows the data points of several depositions of $EuO_{1\pm\delta}$ on Si at RT and at 300 °C. The stoichiometry of the europium oxide films is measured *in situ* by XPS. A sensitive measure of the europium charge state is the valence band spectrum, which is depicted in Fig. 2. Eu^{2+} has a half filled 4f shell while Eu^{3+} contains 6 electrons in the 4f shell. The removal of 1 electron is visible as a shift of the 4f electron removal state to higher binding energies. The data points labeled A to E in Fig. 1 correspond to the spectra in Fig. 2. The XPS spectrum of sample A deposited at 5.2×10^{-6} mbar shows a metallic Fermi edge and has the same spectrum as a pure europium film deposited in UHV. It shows the Eu $4f^7 \rightarrow 4f^6$ electron removal state at a binding energy of 1.9 eV. The spectra of samples B to E show the valence band as a function of increasing oxygen partial pressure. Adding oxygen leads to the vanishing of the Fermi edge and the appearance of the O 2p level. The spectra of samples D and E show a clear contribution of both the $4f^7 \rightarrow 4f^6$ and the $4f^6 \rightarrow 4f^5$ which indicates that both Eu^{2+} and Eu^{3+} are present in the thin film. A further increase of oxygen results in the vanishing of the Eu^{2+} character until only Eu_2O_3 is visible.

Fig. 1 shows the ablation frequency dependence of the EuO stability window position. EuO is formed at 2.5×10^{-6} at 5 Hz and is shifted to 1.0×10^{-6} mbar at an ablation frequency of 20 Hz, directly indicative of a scaling with the Eu flux. Increasing the frequency leads to a higher oxygen partial pressure necessary to obtain EuO. Elevating the temperature provides that the stability window of mono-oxide formation broadens.

It is concluded that it is possible with PLD to deposit Eu metal, and $EuO_{1\pm\delta}$ thin films that are deficient as well as rich in oxygen, in UHV conditions.

3. Magnetization measurements

Fig. 3 shows the magnetization versus temperature of a 70 nm thick $EuO_{1\pm\delta}$ film, capped with a 15 nm Au capping, deposited on an etched Si substrate. The magnetization is determined by normalizing the gross moment to the thickness of the thin film. The magnetic properties were measured with a vibrating sample magnetometer (VSM) option of a Quantum Design physical property measurement system. The film is deposited at an ablation frequency of 5 Hz in a HV system with a background pressure of 5×10^{-7} mbar, containing 0.3 mbar of Argon. The substrate is heated to a temperature of 350 °C during deposition. Fig. 3 contains both the temperature dependent magnetization measured at a fixed field of 5 mT and the temperature dependence of the saturation magnetization determined at 100 mT. The T_C of the film is 70 K and M saturates to the expected value of 7 μ_B per Eu-atom [20]. The magnetization versus temperature of the films shows different behavior at the two background fields. The 100 mT background shows Brillioun like behavior, while the curve measured at 5 mT is non-Brillioun like. The deviation from the Brillioun law is also observed in MBE-grown $EuO_{1\pm\delta}$ [5]. The inset of Fig. 3 shows a hysteresis

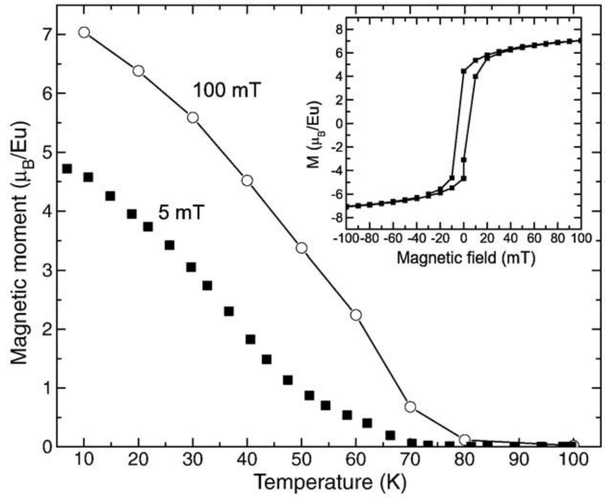

Fig. 3. Magnetization versus temperature of a 70 nm thick $EuO_{1\pm\delta}$ film on Si at two different background fields. The inset shows the hysteresis loop of the magnetization as function of applied field, showing a saturation magnetic moment of 7 μ_B per unit cell. (Solid lines are guides to the eye).

loop measured at 10 K, from which a coercive field of 10 mT can be determined. It is not possible to place the sample of Fig. 3 in Fig. 1, since the sample was capped after deposition for the VSM measurement.

X-ray diffraction on $EuO_{1\pm\delta}$ films, deposited on Si, show both the EuO [111] and [002] peaks. It is expected that deposition at an elevated substrate temperature leads to an enhanced crystallinity of the thin films. In the case of $EuO_{1\pm\delta}$ on Si, however, above 400 °C, intermixing between Eu and Si leads the formation of europium silicide. This is also observed for MBE of EuO films on Si [14].

4. Epitaxial growth of EuO thin films

Integration of EuO with complex oxide material requires epitaxial growth. For epitaxial growth, the perovskite like material $YAlO_3$ is chosen as substrate material. EuO is proven to grow along its [001] direction on $YAlO_3$ [110] and along the [110] direction on $YAlO_3$ [001], see reference [9]. Before deposition, $YAlO_3$ is annealed in oxygen for 5 h at 1000 °C, resulting in a flat surface with terrace-step widths of 200 nm. Europium is ablated in a background pressure of $1–2\times10^{-8}$ mbar at a substrate temperature of 400 °C. In this case oxygen is expected to diffuse from the substrate to the film and no additional oxygen is added. Note also that europium oxide, deposited under the same conditions on silicon, results in metallic europium or europium silicide growth. Growth is monitored *in situ* using reflection high-energy electron diffraction (RHEED). Fig. 4 show the RHEED patterns of the substrate and the europium oxide film, grown at a deposition frequency of 5 Hz. Fig. 4a and b show the two directions of the pseudo-square surface net of $YAlO_3$. Figs 4c and d show the EuO film. From the position of the diffraction spots it is seen that the epitaxial relation is preserved during growth. The pattern itself shows that the film is rough relative to the wavelength of the electron beam, deduced from the transmission features in the pattern. These transmission features show the cubic symmetry in both substrate directions. Note in Fig. 4 that the EuO [001] peak vanishes, which is a characteristic feature of a rocksalt diffraction pattern [19]. *In situ* XPS shows indeed the right europium charge state.

5. Summary

In summary, we have shown that crystalline EuO thin films can be deposited by PLD. We observe that it is possible to form EuO using a Eu metal target and ablate in a UHV and even HV environment, benefitting from the large Eu flux that is characteristic for PLD. *In situ* monitoring the growth of EuO on $YAlO_3$ shows that the thin film grows epitaxially. The stoichiometry of the film is measured using XPS, in which the difference between europium metal, Eu^{2+} and Eu^{3+} is easily distinguished. VSM measurements show that the EuO is ferromagnetic with a T_C around 70 K and a saturation magnetic moment of 7 μ_B per unit cell.

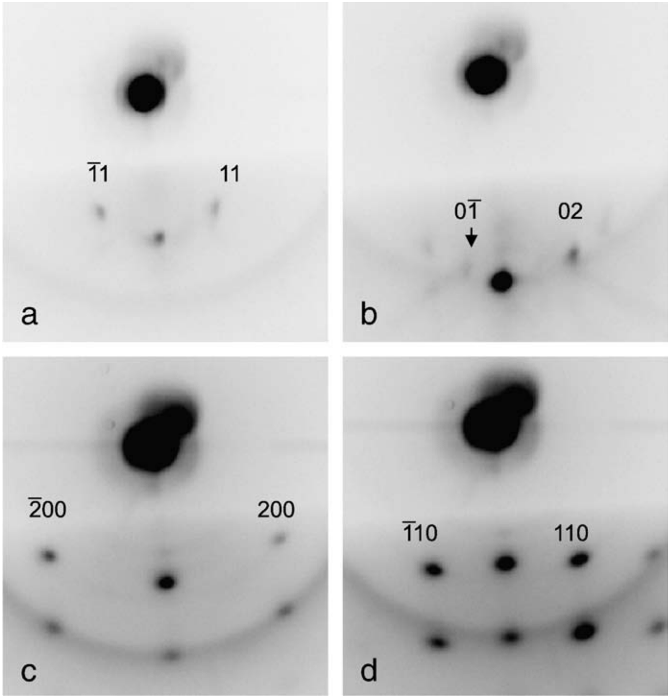

Fig. 4. RHEED-pattern of EuO on $YAlO_3$. a) pattern along the [111] direction of and b) along the [001] direction of bare $YAlO_3$. c) shows the europium oxide film, visible is the [200] direction of the film. d) depicts the [110] orientation of the europium oxide film.

Acknowledgements

Enlightening discussions are acknowledged with J.S. Moodera, T.S. Santos, A. Schmehl, and R. Sutarto. This work is financially supported by the Netherlands Organization for Scientific Research (NWO) through VIDI grants (A.B. and G.R.) and the NanoNed Program.

References

[1] S.J. Pearton, C.R. Abernathy, M.E. Overberg, G.T. Thaler, D.P. Norton, N. Theodoropoulou, A.F. Hebard, Y.D. Park, F. Ren, J. Kim, J. Appl. Phys. 93 (2003) 1.
[2] J.S. Moodera, R. Meservey, X. Hao, Phys. Rev. Lett. 70 (1993) 853.
[3] J.S. Moodera, X. Hao, G.A. Gibson, R. Meservey, Phys. Rev. Lett. 61 (1988) 637.
[4] T.S. Santos, J.S. Moodera, Phys. Rev. B 69 (2004) 241203.
[5] T.S. Santos, J.S. Moodera, K.V. Raman, E. Negusse, J. Holroyd, J. Dvorak, M. Liberati, Y.U. Idzerda, E. Arenholz, Phys. Rev. Lett. 101 (2008) 147201.
[6] P.G. Steeneken, L.H. Tjeng, I. Elfimov, G.A. Sawatzky, G. Ghiringhelli, N.B. Brookes, D.-J. Huang, Phys. Rev. Lett. 88 (2002) 047201.
[7] M. Oliver, J. Dimmock, A. McWhorter, T. Reed, Phys. Rev. B 5 (1972) 1078.
[8] S. Kawabata, J. Phys. Soc. Jap. 70 (2001) 1210.
[9] A. Schmehl, V. Vaithyananthan, A. Herrnberger, S. Thiel, C. Richter, M. Liberati, T. Heeg, M. Röckerath, L. Kourkoutis, S. Mühlbauer, Nat. Mater. 6 (2007) 882.
[10] R. Pangaluri, T.S. Santos, E. Negusse, J. Dvorak, Y. Idzerda, J.S. Moodera, B. Nadgorny, Phys. Rev. B 78 (2008) 125307.
[11] Y. Tomioka, A. Asamitsu, H. Kuwahara, Y. Moritomo, Y. Tokura, Phys. Rev. B 53 (1996) R1689.
[12] Y. Tokura, H. Kuwahara, Y. Moritomo, Y. Tomioka, A. Asamitsu, Phys. Rev. Lett. 76 (1996) 3184.
[13] H. Ott, S.J. Heise, R. Sutarto, Z. Hu, C.F. Chang, H.H. Hsieh, H.-J. Lin, C.T. Chen, L.H. Tjeng, Phys. Rev. B 73 (2006) 094407.
[14] J. Lettieri, V. Vaithyanathan, S.K. Eah, J. Stephens, V. Sih, D.D. Awschalom, J. Levy, D.G. Schlom, Appl. Phys. Lett. 83 (2003) 975.
[15] R. Ulbricht, A. Schmehl, T. Heeg, J. Schubert, D. Schlom, Appl. Phys. Lett. 93 (2008) 102105.

[16] H. Lee, J.-Y. Kim, K.-J. Rho, B.-G. Park, J.-H. Park, J. Appl. Phys. 102 (2007) 053903.

[17] R. Sutarto, S.G. Altendorf, B. Coloru, M. Moretti Sala, T. Haupricht, C.F. Chang, Z. Hu, C. Schussler-Langeheine, N. Hollmann, H. Kierspel, H.H. Hsieh, H.-J. Lin, C.T. Chen, L.H. Tjeng, Phys. Rev. B 79 (2009) 205318.

[18] Y. Wang, M.K. Niranjan, J.D. Burton, J.M. An, K.D. Belashchenko, Y.Y. Tsymbal, Phys. Rev. B. 79 (2009) 212408.

[19] W. Siemons, G. Koster, D.H.A. Blank, R.H. Hammond, T.H. Geballe, M.R. Beasley, Phys. Rev. B. 79 (2009) 212408.

[20] M. Muller, G. Miao, J.S. Moodera, J. Appl. Phys. 105 (2009) 07C917.